

PCCP

Accepted Manuscript



This is an *Accepted Manuscript*, which has been through the Royal Society of Chemistry peer review process and has been accepted for publication.

Accepted Manuscripts are published online shortly after acceptance, before technical editing, formatting and proof reading. Using this free service, authors can make their results available to the community, in citable form, before we publish the edited article. We will replace this *Accepted Manuscript* with the edited and formatted *Advance Article* as soon as it is available.

You can find more information about *Accepted Manuscripts* in the [Information for Authors](#).

Please note that technical editing may introduce minor changes to the text and/or graphics, which may alter content. The journal's standard [Terms & Conditions](#) and the [Ethical guidelines](#) still apply. In no event shall the Royal Society of Chemistry be held responsible for any errors or omissions in this *Accepted Manuscript* or any consequences arising from the use of any information it contains.

Cite this: DOI: 10.1039/c0xx00000x

www.rsc.org/xxxxxx

ARTICLE TYPE

Generation of Free Oxygen Atoms O(³P) in Solution by Photolysis of 4-Benzoylpyridine N-Oxide

Jack M. Carraher^{a,b} and Andreja Bakac^{a,b*}

Received (in XXX, XXX) Xth XXXXXXXXXX 20XX, Accepted Xth XXXXXXXXXX 20XX

DOI: 10.1039/b000000x

Laser flash photolysis of 4-benzoylpyridine N-oxide (BPyO) at 308 nm in aqueous solutions generates a triplet excited state ³BPyO* that absorbs strongly in the visible, λ_{max} 490 and 380 nm. ³BPyO* decays with the rate law k_{decay}/s⁻¹ = (3.3 ± 0.9) × 10⁴ + (1.5 ± 0.2) × 10⁹ [BPyO] to generate a mixture of isomeric hydroxylated benzoylpyridines, BPy(OH), in addition to small amounts of oxygen atoms, O(³P).

Molecular oxygen quenches ³BPyO*, k_Q = 1.4 × 10⁹ M⁻¹ s⁻¹, but the yields of O(³P) increase in O₂-saturated solutions to 36%. Other triplet quenchers have a similar effect, which rules out the observed ³BPyO* as a source of O(³P). It is concluded that O(³P) is produced from either ¹BPyO* or a short-lived, unobserved, higher energy triplet generated directly from ¹BPyO*. ³BPyO* is reduced by Fe²⁺ and by ABTS²⁻ to the radical anion BPyO^{•-} which exhibits a maximum at 510 nm, ε = 2200 M⁻¹ cm⁻¹. The anion engages in back electron transfer with ABTS^{•-} with k = 1.7 × 10⁹ M⁻¹ s⁻¹. The same species can be generated by reducing ground state BPyO with [•]C(CH₃)₂OH. The photochemistry of BPyO in acetonitrile is similar to that in aqueous solutions.

Introduction

Atomic oxygen in its ground triplet state, O(³P), is a powerful but selective oxidant for organic substrates. In the gas phase and in solution it reacts with aromatic hydrocarbons^{1,2} and alkanes^{3,4} to yield alcohols, and with olefins⁵⁻⁹ to yield epoxides, ketones, and aldehydes. By comparison, hydroxyl radicals, ozone and other reactive oxygen species often react with organic compounds almost indiscriminately and generate an array of oxidized, fragmented and isomerized products. The combined selectivity and reactivity of O(³P) suggest that it may be useful as oxidant in laboratory and industry. It is also the least explored of reactive oxygen species in solution, especially in aqueous media.

Detailed reactivity and synthetic studies in solution are limited by lack of convenient and reliable methods for the generation and detection of O(³P). Following leads from gas phase work^{3,6,10} which often utilizes ultraviolet (UV) and vacuum ultraviolet photolysis of suitable precursors (O₂, CO₂, N₂O), most solution studies also relied on UV photolysis to generate O(³P). Oxo-anions (ClO⁻, ClO₃⁻, BrO⁻, BrO₂⁻, BrO₃⁻, IO₄⁻),¹¹ H₂O₂¹² and heterocyclic N-oxides¹³⁻¹⁵ and S-oxides^{4,7,8,16,17} were employed as precursors. Ozone is also a good photochemical source of O(³P),¹⁸ but its use is limited owing to rapid direct reactions with majority of oxidizable substrates. Radiolysis of water¹⁹ and microwave discharge⁸ have also been employed.

Unfortunately, some of these methods also produce other reactive oxygen species such as O(¹D), ¹O₂, O₃, or HO[•] in addition to O(³P).^{11,12,19} Moreover, in none of the solution studies was O(³P) observed directly. Rather, the evidence for it

is based on the observed chemical transformations and on the similarity of the products and reactivity patterns with those of gas-phase O(³P).^{4,15,17}

Heterocyclic N-oxides and S-oxides have received most attention among photochemical O(³P) precursors in solution, but there is a great deal of disagreement regarding the mechanism. The triplet excited state of heterocyclic N-oxides has been suggested to be responsible for photo-deoxygenation, while oxygen migration and ring cleavage are attributed to the excited singlet.^{15,20,21} This hypothesis is supported by an apparent correlation between the degree to which the triplet is formed in substituted pyridine N-oxides and the extent of deoxygenation.^{15,20,22} Also, introduction of O₂, a known triplet quencher, inhibits deoxygenation.^{20,22} On the other hand, energy transfer from triplet benzophenone failed to cause deoxygenation of thiophene S-oxide^{23,24} suggesting that the observed triplet does not eject O(³P). Also, calculations show that the observed triplet thiophene S-oxide is too low in energy for deoxygenation.²⁴ Even the very existence of O(³P) is questioned by some workers who propose an oxaziridine intermediate to be the key to observed chemistry.^{25,26}

In the present study we address some of the questions regarding the mechanism of photochemical O(³P) formation and its involvement in substrate oxidation. For this purpose we chose 4-benzoylpyridine N-oxide (BPyO), a compound for which early studies reported large chemical yields of 4-benzoylpyridine (BPy) and, by implication, of O(³P) upon steady-state photolysis with low-pressure mercury lamp.²² In that work the efficiency of deoxygenation was attributed to fast intersystem crossing (k_{isc} ~ 10¹¹ s⁻¹) that forces the molecule into

triplet manifold, the proposed source of $O(^3P)$.²² Here we describe a time-resolved study of the photochemistry of BPyO to directly detect the triplet excited state and determine its role in $O(^3P)$ formation.

5 Experimental

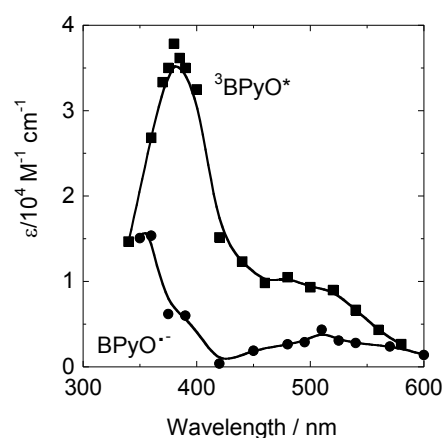
Laser flash photolysis (LFP) experiments were carried out on air-free solutions of BPyO in 1-cm quartz, septum-sealed fluorescence cells. Steady-state irradiations for product analysis utilized a Luzchem LCZ-5 photoreactor with the main wavelength output at 313 nm. Other, undesired bands were blocked with a set of filters consisting of a 30-mL beaker filled with aqueous solution of 1 mM K_2CrO_4 placed inside a larger beaker containing 0.33 M aqueous $CuSO_4$. The sample was placed in the center of the inner beaker, and the levels of filter solutions were brought up to just below the screw cap on the cell. A composite UV-Vis spectrum of the two filters in a 1 cm cell exhibits an absorbance of ≥ 2 at 302 nm and 340 nm as shown in Figure S1.[†] The spectra of BPyO in water and in acetonitrile are also shown in Figure S1. The disappearance of BPyO was observed as a decrease in absorption bands around 300 nm. For NMR analysis, 0.6 mL of 1-2 mM BPyO were irradiated in a 0.1 cm quartz cell. A small amount of 2-PrOH was added as internal standard prior to NMR data collection. As a control, identical solutions were irradiated with 500 laser shots. 1H NMR was identical to that collected after steady-state photolysis.

LFP utilized a Lambda Physik Excimer Pro 2 xenon chloride excimer laser and an Applied Photophysics monitoring system.²⁷ Experiments with $^*UO_2^{2+}$ used a Phasar dye laser²⁸ and LD 490 dye (Exciton). UV-Vis spectra were collected with a Shimadzu UV-3101PC spectrophotometer. NMR spectra were obtained with a Bruker AVIII-600 (600 MHz) and analyzed with MestReNova version 8.1 software. GC-MS data were collected with an Agilent 6890 gas chromatograph equipped with a split/splitless injector (10:1 split ratio). An Agilent HP-PLOT/Q column was attached to a Waters GCT accurate mass time-of-flight mass spectrometer in positive EI mode (70 eV) with a scan rate of 0.3 s per scan and a mass range of 10–200 Daltons. Waters MassLynx 4.0 software was used to acquire and process GC-MS data (average of 3–5 runs). KaleidaGraph 4.0 software was used for data analysis and processing. Water was purified with a Barnstead EASYpure III UV UF system.

Results

Laser flash photolysis of BPyO

The 308-nm excitation of air-free aqueous solutions of BPyO (λ_{max} 292 nm, $\epsilon = 2.0 \times 10^4 M^{-1} cm^{-1}$, Figure S1) yielded a transient assigned as a triplet excited state, $^3BPyO^*$. The UV-Vis spectrum of $^3BPyO^*$ was collected point-by-point and is shown in Figure 1. Molar absorptivities were obtained in experiments with ABTS²⁻ described later. The values at the two maxima are $\epsilon_{380} = (3.5 \pm 0.4) \times 10^4 M^{-1} cm^{-1}$, and $\epsilon_{490} = (1.0 \pm 0.1) \times 10^4 M^{-1} cm^{-1}$. No emission was observed in the 350 - 600 nm range upon excitation of BPyO at room temperature in H_2O or D_2O .



55 **Figure 1.** Absorption spectra of $^3BPyO^*$ in water (squares) and $BPyO^-$ in 0.1 M aqueous $HClO_4$ (circles) under air-free conditions.

$^3BPyO^*$ decays with exponential kinetics, but the first order rate constant exhibits dependence on the concentration of BPyO, $k_{decay}/s^{-1} = (3.3 \pm 0.9) \times 10^4 + (1.5 \pm 0.2) \times 10^9 [BPyO]$, see Figure 2. The two rate constants are associated with the paths in eq 1-2. The kinetics are unaffected by pH or by replacing H_2O with D_2O , but signal intensity diminishes at high $[H^+]$. In the extreme of 6 M $HClO_4$, where $BPyOH^+$ dominates ($K_a = 1.2$, Figures S2-S4), no photochemistry was observed.



$^3BPyO^*$ reacts rapidly with O_2 . A plot of k_{obs} vs. $[O_2]$ for the reaction at 50 μM BPyO in aqueous solution is linear with a slope $k_Q = (1.4 \pm 0.1) \times 10^9 M^{-1} s^{-1}$, and intercept $k_{decay} = 1.2 \times 10^5 s^{-1}$, Figure S6. The value of the intercept is identical to k_{decay} measured at this concentration of BPyO under argon, Figure 2. In acetonitrile, the value of k_Q is $(1.3 \pm 0.2) \times 10^9 M^{-1} s^{-1}$. The long intrinsic lifetime and rapid quenching with O_2 are both characteristic of triplet excited states.²⁹

A number of transition metal complexes also quench $^3BPyO^*$ as shown in Table 1. In every case the reaction follows the rate law $k_{obs} = k_{decay} + k_Q[Q]$, where Q is the quencher and k_{decay} is the sum of the rate constants for reactions 1-2, see above. Except for Fe^{2+} , none of the metal complexes in Table 1 generated observable products. Also, no emission was observed at 720 nm following quenching with *trans*-([14]jane N_4)Cr(CN) $_2^+$, ruling out the formation of the long-lived excited chromium complex.^{30,31}

The photochemical behavior of BPyO in acetonitrile is qualitatively similar to that in water. A triplet excited state, Figure S5, forms in the flash and decays with the same rate law in CH_3CN and CD_3CN , $k_{decay}/s^{-1} = (6.7 \pm 0.1) \times 10^4 s^{-1} + (1.3 \pm 0.1) \times 10^9 [BPyO]$, see Figure 2.

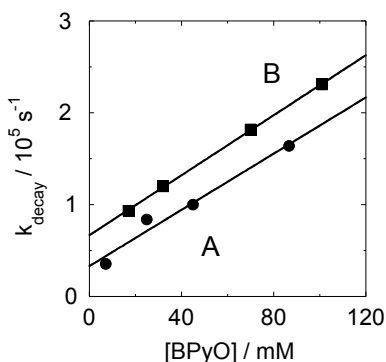
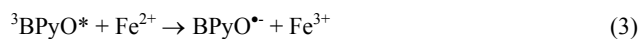


Figure 2. Plot of k_{obs} vs. $[\text{BPyO}]$ for the decay of ${}^3\text{BPyO}^*$ in water (A) and acetonitrile (B).

The ${}^3\text{BPyO}^* / \text{Fe}^{2+}$ reaction was studied in the acidity range $0.1 \text{ M} \leq [\text{H}^+] \leq 1 \text{ M}$ by monitoring the disappearance of ${}^3\text{BPyO}^*$ at 510 nm. The absorbance decreased in two stages. The kinetics of the first step, interpreted as reduction of ${}^3\text{BPyO}^*$ to BPyO^{\bullet} , eq 3, are exponential with the rate constant linearly dependent on Fe^{2+} to yield $k_3 = (1.3 \pm 0.1) \times 10^8 \text{ M}^{-1} \text{ s}^{-1}$, independent of $[\text{H}^+]$, Figures 3-4. As shown in traces b-d of Figure 3, the final absorbance for this stage is the same for all of the concentrations of Fe^{2+} used (3-18 mM) implying complete reduction of ${}^3\text{BPyO}^*$ in every case. The visible spectrum of BPyO^{\bullet} in Figure 1 was obtained under the conditions of trace c in Figure 3. The absorbance of ${}^3\text{BPyO}^*$ was recorded immediately after the flash, and that of the anion 4 μs later when the reduction by 9 mM Fe^{2+} was complete.



At longer times the absorbance at 510 decreases, but the kinetics were too slow ($\gg 100 \mu\text{s}$, slow phase in Figure 3) and the absorbance changes were too small for precise rate measurements with our instrument. Qualitatively, the disappearance of BPyO^{\bullet} seemed independent of $[\text{Fe}^{2+}]$ and $[\text{H}^+]$. Attempts to check for back electron transfer between BPyO^{\bullet} and Fe^{3+} were hampered by small and equal concentrations of both species which leads to slow second-order

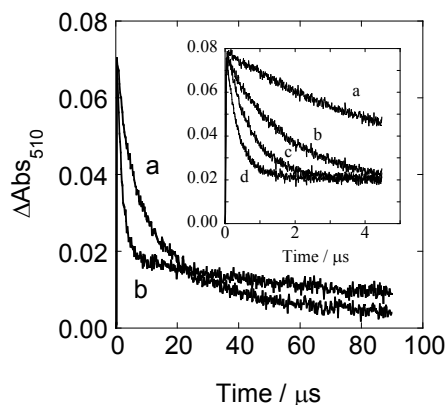


Figure 3. Absorbance decrease at 510 nm following laser flash. Conditions: 43 μM BPyO in 0.1 M HClO_4 in the absence of Fe^{2+} (a), and at $[\text{Fe}^{2+}] = 3 \text{ mM}$ (b). Inset: Expanded traces for the reaction having $[\text{Fe}^{2+}] = 0$ (a), 3 mM (b), 9 mM (c), and 18 mM (d).

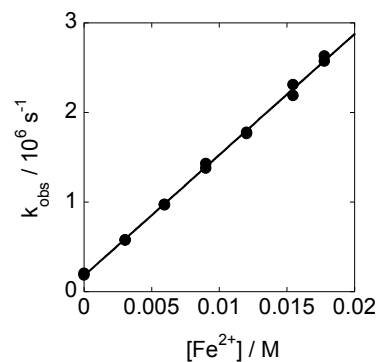
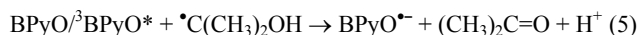
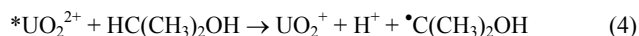


Figure 4. Plot of k_{obs} vs $[\text{Fe}^{2+}]$ for the reaction between ${}^3\text{BPyO}^*$ and Fe^{2+} in 0.10 M HClO_4 .

kinetics. Adding extra Fe^{3+} to accelerate the reaction is ruled out by rapid quenching of ${}^3\text{BPyO}^*$ by Fe^{3+} , Table 1. To provide additional support for electron-transfer in the reaction between ${}^3\text{BPyO}^*$ and Fe^{2+} , eq 3, we searched for other one-electron reductants that are transparent in the visible and that could rapidly reduce BPyO or ${}^3\text{BPyO}^*$. For this purpose we chose ${}^{\bullet}\text{C}(\text{CH}_3)_2\text{OH}$, generated from ${}^*\text{UO}_2^{2+}/\text{CH}(\text{CH}_3)_2\text{OH}$ by the well-established photochemical route.^{32,33}

An air-free solution containing 1 mM UO_2^{2+} , 0.5 M H_3PO_4 , 70 μM BPyO , and 0.5 M 2-PrOH was exposed to a 308 nm flash. Both ${}^*\text{UO}_2^{2+}$ and ${}^3\text{BPyO}^*$ were produced. The concentration of ${}^*\text{UO}_2^{2+}$, and thus $[{}^{\bullet}\text{C}(\text{CH}_3)_2\text{OH}]$, was determined by flashing an otherwise identical solution but without 2-PrOH, and measuring the absorbance at 580 nm where ${}^*\text{UO}_2^{2+}$ exhibits a maximum, $\epsilon = 4500 \text{ M}^{-1} \text{ cm}^{-1}$.³⁴

Under the conditions chosen, all of ${}^*\text{UO}_2^{2+}$ reacts with 2-PrOH to generate ${}^{\bullet}\text{C}(\text{CH}_3)_2\text{OH}$ as in eq 4, $k_4 = 1.4 \times 10^7 \text{ M}^{-1} \text{ s}^{-1}$.³³ Even though BPyO quenches ${}^*\text{UO}_2^{2+}$ ($k = 2.5 \times 10^9 \text{ M}^{-1} \text{ s}^{-1}$, Figure S7), the concentration of BPyO was too low to compete with 2-PrOH for ${}^*\text{UO}_2^{2+}$. The ${}^{\bullet}\text{C}(\text{CH}_3)_2\text{OH}$ produced in reaction 4 should react with BPyO and probably also with ${}^3\text{BPyO}^*$, eq 5. Some ${}^{\bullet}\text{C}(\text{CH}_3)_2\text{OH}$ will be lost in the competing self-reactions of eq 6.³⁵



The above experiment was repeated at several wavelengths and the absorbance was recorded as soon as stable reading was reached, about 20 μs . The spectrum so obtained shows a broad maximum around 510 nm, in excellent qualitative agreement with the spectrum obtained in the ${}^3\text{BPyO}^*/\text{Fe}^{2+}$ reaction, Figure 5. The molar absorptivities, obtained by dividing experimental absorbances by independently determined concentration of ${}^*\text{UO}_2^{2+}$ (25 μM) was somewhat lower than those obtained in Fe^{2+} experiments, consistent with some losses in the self-reaction of eq 6. Spectrum b in Figure 5 was obtained by multiplying the experimental spectrum by a factor of 1.4 so as to bring ϵ_{510} to $2.2 \times 10^3 \text{ M}^{-1} \text{ cm}^{-1}$, the value determined in Fe^{2+} experiments. The combination of this factor and the known k_6 ($5 \times 10^8 \text{ M}^{-1} \text{ s}^{-1}$)³⁵ provides an estimate for the rate constant for $\text{BPyO}/{}^{\bullet}\text{C}(\text{CH}_3)_2\text{OH}$ reaction, $k_5 \sim 10^9 \text{ M}^{-1} \text{ s}^{-1}$.

Table 1. Second-Order Rate Constants for Quenching of ${}^3\text{BPyO}^*$ ^a

| Quencher | $k_Q / \text{M}^{-1} \text{s}^{-1}$ |
|--|-------------------------------------|
| Ag^{+b} | $5.8 (\pm 0.1) \times 10^6$ |
| Mn^{2+b} | $2.3 (\pm 0.1) \times 10^7$ |
| Ni^{2+} | $6.5 (\pm 0.1) \times 10^7$ |
| $(\text{Me}_{10}\text{-}([14]\text{aneN}_4)\text{Ni}^{2+c})$ | $7.5 (\pm 0.4) \times 10^7$ |
| $(\text{Me}_4\text{-}[14]\text{aneN}_4)\text{Ni}^{2+c}$ | $1.6 (\pm 0.1) \times 10^8$ |
| $([14]\text{aneN}_4)\text{Cr}(\text{CN})_2^{+g}$ | $4.0 (\pm 0.1) \times 10^8$ |
| $(\text{Me}_6\text{-}[14]\text{aneN}_4)\text{Ni}^{2+h}$ | $4.4 (\pm 0.1) \times 10^8$ |
| $([14]\text{aneN}_4)\text{Ni}^{2+g}$ | $1.7 (\pm 0.1) \times 10^9$ |
| Fe^{2+b} | $1.2 (\pm 0.1) \times 10^8$ |
| Fe^{2+d} | $1.3 (\pm 0.1) \times 10^8$ |
| Cu^{2+f} | $1.7 (\pm 0.1) \times 10^8$ |
| Fe^{3+f} | $2.5 (\pm 0.1) \times 10^8$ |
| Pd^{2+b} | $4.8 (\pm 0.1) \times 10^9$ |
| $\text{O}_2^{i,j}$ | $1.3 (\pm 0.1) \times 10^9$ |
| O_2 | $1.4 (\pm 0.1) \times 10^9$ |
| ABTS^{2-k} | $4.1 (\pm 0.1) \times 10^9$ |
| I^{-i} | $2.2 (\pm 0.1) \times 10^9$ |
| I^{\cdot} | $5.0 (\pm 0.1) \times 10^9$ |
| MeOH | $<10^4^d$ |
| 2-PrOH | $<10^4^d$ |

^a $\lambda_{\text{exc}} = 308 \text{ nm}$, $\lambda_{\text{mon}} = 510 \text{ nm}$. Conditions: $50 \mu\text{M BPyO}$, no added acid unless noted, 25°C . Metal ions shown without specific ligands are aqua-species. ^b 0.1 M HClO_4 . ^c $\text{Me}_{10}\text{-}([14]\text{aneN}_4) = (1\text{R},4\text{R},8\text{S},11\text{S})\text{-C-meso-1,4,5,5,7,8,11,12,12,14-decamethyl-1,4,8,11-tetraazacyclotetradecane}$. ^d 1.0 M HClO_4 . ^e $\text{Me}_4\text{-}[14]\text{aneN}_4 = (1\text{R},4\text{S},8\text{R},11\text{S})\text{-1,4,8,11-tetramethyl-1,4,8,11-tetraazacyclotetradecane}$. ^f 1 M HClO_4 . ^g $[14]\text{aneN}_4 = 1,4,8,11\text{-tetraazacyclotetradecane}$. ^h $\text{Me}_6\text{-}[14]\text{aneN}_4 = \text{meso-5,5,7,12,12,14-hexamethyl-1,4,8,11-tetraazacyclotetradecane}$. ⁱ In acetonitrile. ^j Taking $[\text{O}_2] = 11.3 \text{ mM}$ in O_2 -saturated acetonitrile. ^k $\lambda_{\text{mon}} = 417 \text{ nm}$

As shown in Figure 6, laser flash photolysis of solutions containing BPyO and ABTS^{2-} causes a jump in absorbance corresponding to the formation of ${}^3\text{BPyO}^*$, followed by exponential increase that yields the spectrum of $\text{ABTS}^{\cdot-}$. Finally, $\text{ABTS}^{\cdot-}$ disappears with second-order kinetics that become exponential when the reaction is run in the presence of excess $\text{ABTS}^{\cdot-}$.

The kinetics of formation of $\text{ABTS}^{\cdot-}$ were determined in a limited range of $[\text{ABTS}^{2-}]$, $30 - 90 \mu\text{M}$. The upper limit is determined by the strong ABTS^{2-} absorption at the irradiating wavelength, and the lower limit by our desire to keep ABTS^{2-} in a pseudo-first order excess. A plot of k_{obs} against $[\text{ABTS}^{2-}]$ is

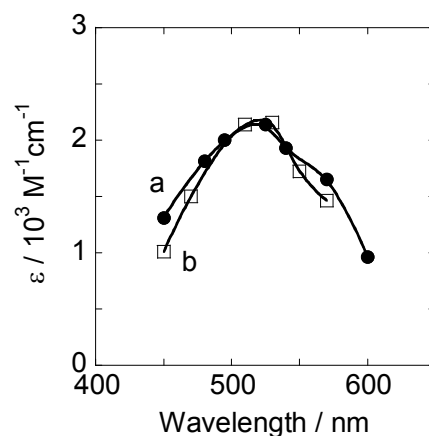
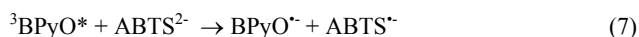


Figure 5. Absorption spectrum of BPyO^* generated by laser flash photolysis of a solution of (a) $50 \mu\text{M BPyO} + 9 \text{ mM Fe}^{2+}$ in 0.1 M HClO_4 and (b) $70 \mu\text{M BPyO} + 1 \text{ mM UO}_2^{2+} + 0.5 \text{ M 2-PrOH}$ in $0.5 \text{ M H}_3\text{PO}_4$. Spectrum (b) was multiplied by a factor of 1.4 to account for loss of ${}^{\cdot}\text{C}(\text{CH}_3)_2\text{OH}$ in self reactions.

linear with $k = (4.1 \pm 0.1) \times 10^9 \text{ M}^{-1} \text{ s}^{-1}$, Figure S8. The linear dependence on $[\text{ABTS}^{2-}]$, and the observation that photolysis of ABTS^{2-} alone causes no absorbance changes in the visible confirm that redox reaction between ${}^3\text{BPyO}^*$ and ABTS^{2-} is responsible for the formation of $\text{ABTS}^{\cdot-}$. By implication, BPyO^* is also produced, eq 7.



The second-order disappearance of $\text{ABTS}^{\cdot-}$ in the next step suggests back electron transfer of eq 8. The fit to second order kinetics yielded $k_8 = 1.8 \times 10^9 \text{ M}^{-1} \text{ s}^{-1}$. When the experiment was run in the presence of added $\text{ABTS}^{\cdot-}$ ($7 - 22 \mu\text{M}$), the plot of pseudo-first order rate constants against $[\text{ABTS}^{\cdot-}]$ yielded $k_8 = (1.7 \pm 0.3) \times 10^9 \text{ M}^{-1} \text{ s}^{-1}$, Figure S9, in excellent agreement with the above value. Control experiments showed that $\text{ABTS}^{\cdot-}$ does not quench ${}^3\text{BPyO}^*$. The plot in Figure S9 also exhibits an intercept, $(8 \pm 6) \times 10^3 \text{ s}^{-1}$, associated with the decay of $\text{BPyO}^{\cdot-}$. The low value is consistent with the slow decay of $\text{BPyO}^{\cdot-}$ obtained in ${}^3\text{BPyO}^*/\text{Fe}^{2+}$ reaction, Fig. 3.



The reaction of ${}^3\text{BPyO}^*$ with ABTS^{2-} provided a convenient route to molar absorptivities of ${}^3\text{BPyO}^*$. This was done at 417 nm , where $\text{ABTS}^{\cdot-}$ has $\epsilon = 3.47 \times 10^4 \text{ M}^{-1} \text{ cm}^{-1}$.³⁶ As illustrated in Figure 6, flash photolysis experiments provide absorption data for both ${}^3\text{BPyO}^*$ and $\text{ABTS}^{\cdot-}$ derived from it. The measured concentration of $\text{ABTS}^{\cdot-}$ and 1:1 stoichiometry of eq 7 lead to $\epsilon_{417} = (1.5 \pm 0.1) \times 10^4 \text{ M}^{-1} \text{ cm}^{-1}$ for ${}^3\text{BPyO}^*$. The contribution from $\text{BPyO}^{\cdot-}$ was negligible ($\epsilon_{417} \sim 200 \text{ M}^{-1} \text{ cm}^{-1}$). The remainder of ${}^3\text{BPyO}^*$ spectrum was normalized to the 417-nm value.

The ${}^3\text{BPyO}^*/\text{ABTS}^{2-}$ reaction in acetonitrile qualitatively resembled that in water, but low solubility of $(\text{NH}_4)_2\text{ABTS}$ in CH_3CN (about $28 \mu\text{M}$) hindered quantitative work and prevented us from utilizing the reaction with ABTS^{2-} to determine the concentration of excited state in this solvent. Instead, the spectrum was collected by LFP and the lower limit of molar absorptivities was estimated by measuring the absorbed

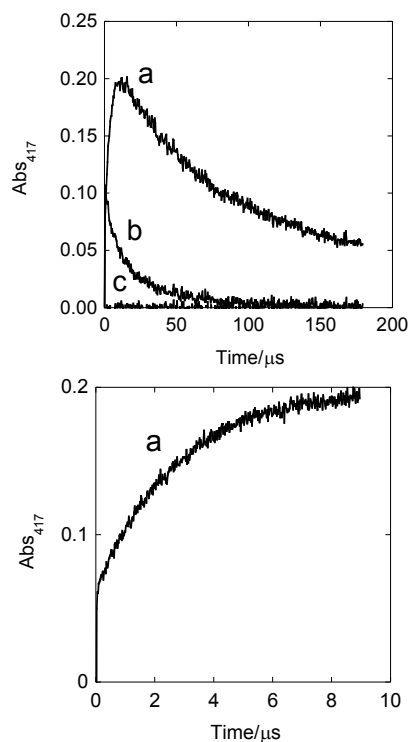


Figure 6. Absorbance changes at 417 nm following laser flash photolysis of air-free aqueous solutions of BPyO and ABTS^{2-} . Top: (a) $40 \mu\text{M BPyO} + 50 \mu\text{M ABTS}^{2-}$; (b) $40 \mu\text{M BPyO}$; (c) $50 \mu\text{M ABTS}^{2-}$. Bottom: initial part of trace a, expanded.



light by $\text{Ru}(\text{bpy})_3^{2+}$ actinometry, see SI, and taking $\Phi(^3\text{BPyO}^*) \leq 1$. This yielded $\epsilon \geq (4.3 \pm 0.9) \times 10^3 \text{ M}^{-1} \text{ cm}^{-1}$ at the 490-nm maximum for $^3\text{BPyO}^*$ in MeCN. In aqueous solution the combination of actinometry and ABTS^{2-} redox chemistry yielded $\Phi(^3\text{BPyO}^*) = 0.2$.

Products

The photolysis of 0.1 mM BPyO in water or acetonitrile for several minutes at 313 nm causes complete disappearance of the 292 nm band as shown in Figures 7 and S10. The final spectrum in water exhibits a maximum near 260 nm with a molar absorptivity of $\sim 8 \times 10^3 \text{ M}^{-1} \text{ cm}^{-1}$, similar to the spectrum of 4-benzoyl pyridine (BPy, $\lambda_{\text{max}} 263 \text{ nm}$, $\epsilon = 1.1 \times 10^4 \text{ M}^{-1} \text{ cm}^{-1}$). However, there are clear differences between the two spectra, Figure 8. The photolysis product absorbs less intensely in the 260-nm region, and more intensely above 320 nm with tailing into the visible.

GC-MS analysis of irradiated solutions of BPyO in both H_2O and MeCN shows the presence of five new isomers of BPyO ($m/z 199.20$). As shown below, these were assigned as hydroxylated BPy on the basis of $^1\text{H NMR}$. Unreacted BPyO and trace amounts of BPy were also observed.

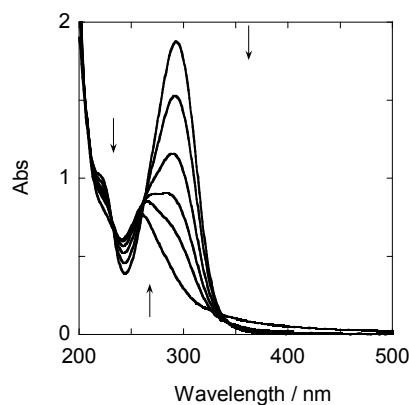


Figure 7. UV-vis spectra (1 cm) of degassed $95 \mu\text{M BPyO}$ in water collected after each 60-second irradiation interval. Final spectrum was collected after an additional 10 minutes of photolysis.

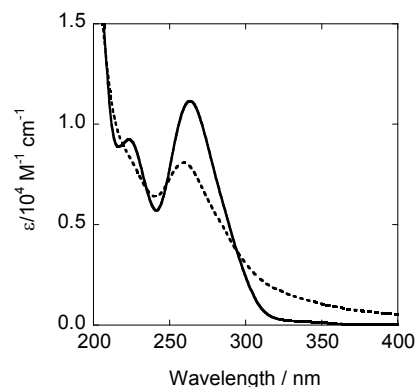


Figure 8. UV spectra of BPy (full line) and product of BPyO photolysis (dashed line) in H_2O .

$^1\text{H NMR}$ spectra of BPyO, BPy and photolysis products are shown in Figures 9 and S11-S13. The most straightforward feature that distinguishes BPyO from BPy is the large difference in chemical shifts of C-H hydrogens next to nitrogen. Thus a simple transformation of BPyO to BPy would have the doublet at 8.49 ppm shift to 8.69 ppm, in addition to other changes in the 7.5 - 8.0 ppm range. As shown in Figure 9, the 8.69 ppm resonance is not observed. Instead, there is a new doublet at 8.77 ppm, assigned as $\alpha\text{-CH}$ of one or more hydroxylated benzoylpyridines along with a number of new, sometimes overlapping resonances in the 7.5 - 8 ppm range. Identical spectra were obtained for solutions that were irradiated under argon and under O_2 . This is as expected at the high concentrations of BPyO (1-2 mM) because intrinsic and self-quenching (eq 1-2) dominate so that only a small fraction of the excited state reacts with O_2 . The combination of data in D_2O and in CD_3CN , where O-H resonances can be observed, made it possible to assign the individual peaks, see SI. It is found that no more than 4% of reacted BPyO was deoxygenated to BPy under our conditions. The remaining products are various isomers of hydroxylated BPy.

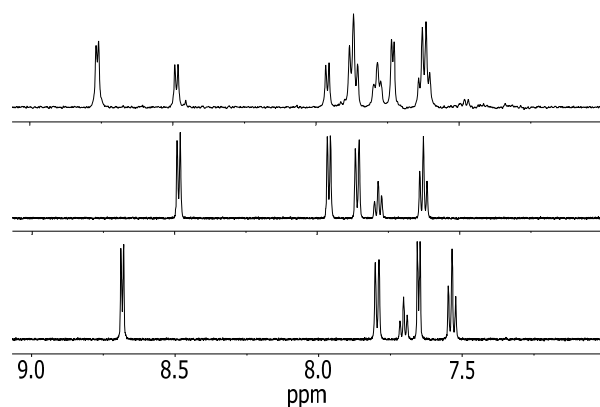


Figure 9. Top: ^1H NMR spectrum of a solution obtained by photolysis (85% completion) of 1.3 mM BPyO in D_2O . Middle: genuine BPyO. Bottom: genuine BPy.

5 Effect of triplet quenchers

The presence of triplet quenchers during photolysis inhibits the loss of BPyO provided the concentration of the quencher is sufficiently high to compete with reactions 1 and 2. This is shown by the plot of the loss of BPyO against irradiation time for solutions containing oxygen or iodide, Figure 10. The concentration of I^- was kept low to eliminate the possibility of direct photolysis which would generate I_3^- and complicate results. At the concentration used, there was no evidence for even traces of I_2/I_3^- in photochemical experiments in the presence of BPyO or in the control that had no BPyO.

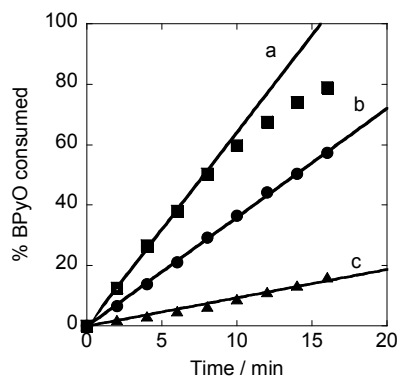


Figure 10. Plot of % BPyO consumed (initial concentration 62 μM) vs. irradiation time in the absence of quencher (a) and in the presence of 0.2 mM I^- (b) or 1.26 mM O_2 (c).

The trend in the slopes in Figure 10 can be rationalized by considering individual contributions to the quenching rates of $^3\text{BPyO}^*$ under each set of conditions. Taking into account the quenching rate constants in Table 1 and concentrations used, one finds that the self-quenching of eq 1-2 ($k = 1.2 \times 10^5 \text{ s}^{-1}$) contributes twice as much to overall quenching in the experiment with O_2 as it does in the experiment with iodide. The results in Figure 10 suggest that major losses of BPyO occur in the process of self-quenching and/or intrinsic decay, whereas triplet quenchers regenerate ground state BPyO and lower the yield of hydroxylated BPy and other products. This is why BPyO disappears more rapidly in the absence of quenchers, and survives the longest in the presence of O_2 , the faster of the two quenchers under chosen conditions.

Search for $\text{O}(^3\text{P})$

To establish whether photolysis of BPyO generates $\text{O}(^3\text{P})$, a series of experiments were conducted with mixtures of BPyO and cyclopentene (5.6 mM, saturation level in water) which is known to react with $\text{O}(^3\text{P})$ to produce ethylene, eq 11, which can be easily detected by GC. The efficiency of C_2H_4 production is 24%.^{3,19} Cyclopentene does not react with O_2 or I^- , does not quench $^3\text{BPyO}^*$, and is not directly photolyzed under our conditions.

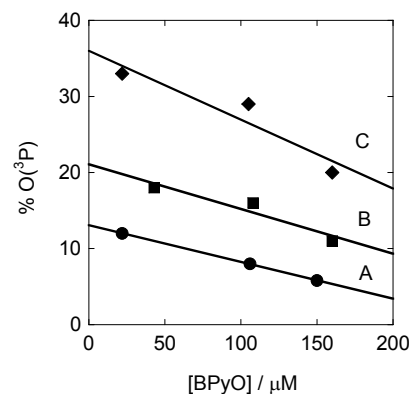


Figure 11. Percentage of consumed BPyO that produced $\text{O}(^3\text{P})$. All solutions contained 5.6 mM $c\text{-C}_5\text{H}_8$. Conditions: (A) Air-free (argon); (B) 0.5 mM I^- under argon; (C) Oxygen-saturated.

The yield of C_2H_4 , taken to be equivalent to 24% of $\text{O}(^3\text{P})$, decreased with increasing $[\text{BPyO}]$ in the range 10 – 160 μM , Figure 11, probably as a result of self-quenching, eq 2, an ever-present background reaction. We rule out a competition between BPyO and cyclopentene for $\text{O}(^3\text{P})$ given the large excess of cyclopentene and the rate constant for $\text{O}(^3\text{P})/\text{cyclopentene}$ reaction of $1.6 \times 10^{10} \text{ M}^{-1} \text{ s}^{-1}$.¹³ Thus more meaningful information regarding $\text{O}(^3\text{P})$ involvement is provided by the intercepts in Figure 11, i. e. at $[\text{BPyO}] = 0$. The largest yield of ethylene and, by implication, of $\text{O}(^3\text{P})$ is obtained in O_2 -saturated solutions where a significant fraction of triplet is quenched by O_2 to regenerate ground state BPyO. In the absence of quenchers, $^3\text{BPyO}^*$ undergoes intrinsic decay (eq 1) which clearly leads to some loss of BPyO and production of BPy(OH), allowing fewer photochemical cycles for a given initial concentration of BPyO, see Figure 10.

Iodide at 0.5 mM should quench $^3\text{BPyO}^*$ even faster than O_2 does (Table 1), and should lead to even greater yields of $\text{O}(^3\text{P})$. We suggest that this is indeed what happens, and that the smaller measured yields of ethylene in iodide solutions are a result of scavenging of some $\text{O}(^3\text{P})$ by iodide in competition with $c\text{-C}_5\text{H}_8$. The relevant rate constants are not known in water, but in acetonitrile¹³ $\text{O}(^3\text{P})$ reacts with $c\text{-C}_5\text{H}_8$ ($k = 1.6 \times 10^{10} \text{ M}^{-1} \text{ s}^{-1}$) faster than with O_2 ($4.1 \times 10^9 \text{ M}^{-1} \text{ s}^{-1}$) but slower than with halides ($5.8 \times 10^{10} \text{ M}^{-1} \text{ s}^{-1}$ (Cl $^-$) and $2 \times 10^{11} \text{ M}^{-1} \text{ s}^{-1}$ (Br $^-$)). The reaction with I^- is expected to be similar to that for Br $^-$. If we assume that the values in water are similar to those in acetonitrile, then under our conditions in oxygen-containing solutions the great majority of $\text{O}(^3\text{P})$ will react with $c\text{-C}_5\text{H}_8$ and only traces of $\text{O}(^3\text{P})$ will be lost in the reaction with O_2 . Iodide

at 0.5 mM, on the other hand, is a strong competitor and could consume about half of $O(^3P)$ generated. Indeed, the amount of C_2H_4 observed in the presence of 0.5 mM I^- is about one half of the amount observed under O_2 , supporting our hypothesis.

5 DMSO as $O(^3P)$ trap

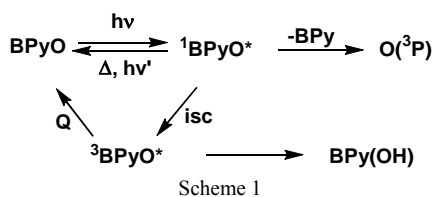
Small concentrations of DMSO decrease the rate of $^3BPyO^*$ decay in water until a constant value of $7.1 (\pm 0.2) \times 10^4 s^{-1}$ is reached at 50 mM DMSO. No further changes are observed at up to 1M DMSO, Figure S14. This observation suggests an interaction between BPyO and DMSO that saturates at 50 mM DMSO, although the nature of the interaction is not clear. There are no changes in 1H NMR of BPyO in the presence of up to 0.1 M DMSO. The behavior in acetonitrile is similar to that in water.

The photolysis of BPyO/DMSO mixtures generated $DMSO_2$ during the early stages, but at higher conversions other products began to form. These include methylsulfonic and methylsulfinic acids as well as ethane and some methane. These secondary products are indicative of the involvement of hydroxyl radicals³⁷ which we believe are formed by photodegradation of the initially produced hydroxypyridines, BPy(OH).³⁸ This hypothesis was checked by photolyzing 1.5 mM BPyO in water to 35% completion to build up BPy(OH). At this point DMSO (0.2 M) was added and the solution was photolyzed to 75 % completion. The products now consisted of mostly sulfinic and sulfonic acids and very little $DMSO_2$, confirming that hydroxypyridines are the major source of hydroxyl radicals.

Discussion

The first observed intermediate following laser photolysis of BPyO is identified as $^3BPyO^*$ on the basis of its long lifetime,²⁹ intense visible spectrum similar to $^3BP^*$,^{39,40} and $^3BPy^*$,^{41,42} and reactivity toward oxygen²⁹ and other triplet quenchers.

Photolysis products are mainly hydroxylated benzoylpyridines, BPy(OH), along with some oxygen atoms, $O(^3P)$. The outcome changes in the presence of triplet quenchers which slow the loss of BPyO and increase chemical yields of $O(^3P)$. These observations clearly show that $^3BPyO^*$ lies on the path to BPy(OH) but not on the path to $O(^3P)$. The latter must be formed from a different intermediate, and prior to $^3BPyO^*$ in the course of photochemical events. The most obvious candidate is the singlet excited state $^1BPyO^*$, as shown in Scheme 1.



According to this proposal, $O(^3P)$ is generated in competition with intersystem crossing (isc) to $^3BPyO^*$. Two major channels for the loss of $^3BPyO^*$ are isomerization to BPy(OH) as in eq 1 and 2, and relaxation to BPyO. In the presence of triplet quenchers, the relaxation is greatly enhanced at the expense of isomerization so that the BPyO- $^1BPyO^*$ - $^3BPyO^*$ -BPyO cycle is repeated many times, each time generating some $O(^3P)$. The

percentage of $^1BPyO^*$ that eliminates $O(^3P)$ is probably small, but under conditions of efficient triplet quenching and multiple photochemical turnovers it leads to an accumulated yield of $O(^3P)$ of 36%.

The elimination of $O(^3P)$ from $^1BPyO^*$ is spin-forbidden which raises the question of mechanism. One possibility is an initial electron transfer to generate $\{BPy^{+}, O^-\}$ followed by rapid back electron transfer yielding $\{BPy, ^3O\}$ and separation of products.²⁴ This mechanism is a variant⁴³ of the commonly observed group or atom transfer initiated by electron transfer. Also, electron transfer followed by its reverse provides, in general, an efficient quenching route for excited states.^{44,45} This mechanism may be particularly relevant for $^3BPyO^*$ which is thought to be better described as an internal charge-transfer state than an $n\pi^*$ absorption.²²

It is also possible that $O(^3P)$ is eliminated from a short-lived, unobserved, higher energy triplet generated directly from $^1BPyO^*$ as an intermediate on route to observed $^3BPyO^*$. Recent computational studies support such a scenario for thiophene S-oxides²⁴ and implicate the unobserved T_2 excited state in S-O scission. As long as the initial triplet BPyO is short lived, similar to $T_2(\pi\pi^*)$ of benzophenone which has $\tau_0 = 10$ ps,⁴⁶ the effect of millimolar concentrations of O_2 would be negligible, consistent with our observations.

An earlier study²² reported 80% deoxygenation of BPyO under irradiation with low pressure mercury lamp (λ_{irr} 254 nm), but it has not been shown that the reaction actually generated $O(^3P)$. Based on O_2 effect and sensitization experiments with biacetyl, that study concluded that deoxygenation of BPyO takes place from a triplet state. The high concentrations of BPyO (0.01 M) and short irradiation wavelength (254 nm) used in that work make the comparison with our study less than straightforward. None the less, the inhibiting effect of oxygen is difficult to rationalize given the short expected lifetime of the initially produced triplet as mentioned above, and the surprising, beneficial effect of oxygen in the present study which rules out the long-lived, observed $^3BPyO^*$ as a source of $O(^3P)$.

Oxygen migration from N-O to the ring carbon(s) to generate BPy(OH) is often assumed to take place intramolecularly. Such a process appears straightforward for insertion at positions adjacent to pyridine nitrogen, but more remote sites would require several migrations. It seems more plausible that some of the products were generated in an intermolecular reaction between $O(^3P)$ and BPyO, or between $^3BPyO^*$ and BPyO, similar to hydroxylation of aromatic solvents by photolysis of benzothiophenes and related compounds.^{4,15,17} Even though the reaction of $O(^3P)$ with benzene has a rate constant of only about $3 \times 10^8 M^{-1}s^{-1}$,¹³ and the reaction with BPyO or BPy may not be much faster, this still appears to be a feasible reaction in the absence of added substrates. The alternative dimerization of $O(^3P)$ to generate O_2 , or recombination with BPy to regenerate BPyO may not provide a much better option owing to the low concentrations of respective reagents. Of course, when the reaction is carried out in the presence of cyclopentene, the combination of the large rate constant and cyclopentene concentrations leads to complete scavenging of $O(^3P)$, so that the observed 36% yield is believed to represent the total amount available under our conditions.

Acknowledgement

This work was supported by the U.S. Department of Energy (DOE), Office of Science, Basic Energy Sciences, Chemical Sciences, Geosciences, and Biosciences Division. The research was performed at the Ames Laboratory which is operated for the U.S. DOE by Iowa State University under contract DE-AC02-07CH11358.

Notes and references

- ¹⁰ ^a Chemistry Department and ^bAmes Laboratory, Iowa State University, Ames, IA 50011, U. S. Fax: 1-515-294-4709; Tel: 1-515-294-3544; Email: bakac@iastate.edu
- † Electronic Supplementary Information (ESI) available: Figures S1-S14 and additional experimental detail.
- 15 (1) Nicovich, J. M.; Gump, C. A.; Ravishankara, A. R. *J. Phys. Chem.* **1982**, *86*, 1690.
- (2) Nicovich, J. M.; Gump, C. A.; Ravishankara, A. R. *J. Phys. Chem.* **1982**, *86*, 1684.
- (3) Cvetanovic, R. J.; Ring, D. F.; Doyle, L. C. *J. Phys. Chem.* **1971**, *75*, 3056.
- (4) Lucien, E.; Greer, A. *J. Org. Chem.* **2001**, *66*, 4576.
- (5) Gaffney, J. S.; Atkinson, R.; Pitts, J. N. *J. Am. Chem. Soc.* **1975**, *97*, 5049.
- (6) Lee, S. Y.; Yoo, H. S.; Kang, W. K.; Jung, K.-H. *Chem. Phys. Lett.* **1996**, *257*, 415.
- 25 (7) Zadok, E.; Rubinraut, S.; Mazur, Y. *J. Org. Chem.* **1987**, *52*, 385.
- (8) Tanner, D. D.; Kandamarachchi, P.; Das, N. C.; Brausen, M.; Vo, C. T.; Camaioni, D. M.; Franz, J. A. *J. Org. Chem.* **1998**, *63*, 4587.
- 30 (9) Thomas, K. B.; Greer, A. *J. Org. Chem.* **2003**, *68*, 1886.
- (10) Nishida, S.; Takahashi, K.; Matsumi, Y.; Taniguchi, N.; Hayashida, S. *J. Phys. Chem. A* **2004**, *108*, 2451.
- (11) Klaning, U. K.; Sehested, K.; Wolff, T. *J. Chem. Soc., Faraday Trans. 1* **1984**, *80*, 2969.
- 35 (12) Sauer, M. C., Jr.; Brown, W. G.; Hart, E. J. *J. Phys. Chem.* **1984**, *88*, 1398.
- (13) Bucher, G.; Scaiano, J. C. *J. Phys. Chem.* **1994**, *98*, 12471.
- (14) Scaiano, J. C.; Bucher, G.; Barra, M.; Weldon, D.; Sinta, R. *J. Photochem. Photobiol. A* **1996**, *102*, 7.
- 40 (15) Albin, A.; Alpegiani, M. *Chem. Rev.* **1984**, *84*, 43.
- (16) Nag, M.; Jenks, W. S. *J. Org. Chem.* **2004**, *69*, 8177.
- (17) Wan, Z.; Jenks, W. S. *J. Am. Chem. Soc.* **1995**, *117*, 2667.
- (18) Reisz, E.; Schmidt, W.; Schuchmann, H.-P.; von Sonntag, C. *Environ. Sci. Technol.* **2003**, *37*, 1941.
- 45 (19) Brown, W. G.; Hart, E. J. *J. Phys. Chem.* **1978**, *82*, 2539.
- (20) Bellamy, F.; Barragan, L. G. R.; Streith, J. *J. Chem. Soc., Chem. Commun.* **1971**, 456.
- (21) Tokumura, K.; Matsushita, Y. *J. Photochem. Photobiol. A* **2001**, *140*, 27.
- 50 (22) Albin, A.; Fasani, E.; Frattini, V. *J. Photochem.* **1987**, *37*, 355.
- (23) de Lucas, N. C.; Albuquerque, A. C. C.; Santos, A. C. A. S.; Garden, S. J.; Nicodem, D. E. *J. Photochem. Photobiol. A* **2007**, *188*, 293.
- 55 (24) Stoffregen, S. A.; Lee, S. Y.; Dickerson, P.; Jenks, W. S. *Photochem. Photobiol. Sci.* **2014**, *13*, 431.
- (25) Spence, G. G.; Taylor, E. C.; Buchardt, O. *Chem. Rev.* **1970**, *70*, 231.
- (26) Daniels, J. S.; Chatterji, T.; MacGillivray, L. R.; Gates, K. S. *J. Org. Chem.* **1998**, *63*, 10027.
- 60 (27) Jee, J.-E.; Bakac, A. *J. Phys. Chem. A* **2010**, *114*, 2136.
- (28) Connolly, P.; Espenson, J. H.; Bakac, A. *Inorg. Chem.* **1986**, *25*, 2169.
- (29) Turro, N. J. *Modern Molecular Photochemistry*; Benjamin/Cummings Publishing Co.: Menlo Park, 1978.
- 65 (30) Kane-Maguire, N. A. P.; Crippen, W. S.; Miller, P. K. *Inorg. Chem.* **1983**, *22*, 696.
- (31) Bakac, A.; Espenson, J. H. *J. Phys. Chem.* **1993**, *97*, 12249.
- (32) Hill, R. J.; Kemp, T. J.; Allen, D. M.; Cox, A. *J. Chem. Soc., Faraday Trans. 1* **1974**, *70*, 847.
- 70 (33) Wang, W.-D.; Bakac, A.; Espenson, J. H. *Inorg. Chem.* **1995**, *34*, 6034.
- (34) Bakac, A.; Burrows, H. D. *Appl. Spectroscopy* **1997**, *51*, 1916.
- 75 (35) Neta, P.; Grodkowski, J.; Ross, A. B. *J. Phys. Chem. Ref. Data* **1996**, *25*, 709.
- (36) Scott, S. L.; Chen, W. J.; Bakac, A.; Espenson, J. H. *J. Phys. Chem.* **1993**, *97*, 6710.
- (37) Veltwisch, D.; Janata, E.; Asmus, K.-D. *J. Chem. Soc., Perkin Trans. 2* **1980**, 146.
- 80 (38) Stapleton, D. R.; Konstantinou, I. K.; Karakitsou, A.; Hela, D. G.; Papadaki, M. *Chemosphere* **2009**, *77*, 1099.
- (39) Bensasson, R. V.; Gramain, J. C. *J. Chem. Soc., Faraday Trans. 1* **1980**, *76*, 1800.
- 85 (40) Ledger, M. B.; Porter, G. *J. Chem. Soc., Faraday Trans. 1* **1972**, *68*, 539.
- (41) Görner, H. *Chem. Phys.* **2008**, *344*, 264.
- (42) Nelson, D. A.; Hayon, E. *J. Phys. Chem.* **1972**, *76*, 3200.
- (43) Sako, M.; Shimada, K.; Hirota, K.; Maki, Y. *J. Am. Chem. Soc.* **1986**, *108*, 6039.
- 90 (44) Jammoul, A.; Dumas, S.; D'Anna, B.; George, C. *Atmospheric Chemical Physics* **2009**, *9*, 4229.
- (45) Hoffman, M. Z.; Bolletta, F.; Moggì, L.; Hug, G. L. *J. Phys. Chem. Ref. Data* **1989**, *18*, 219.
- 95 (46) Aloiese, S.; Ruckebusch, C.; Blanchet, L.; Rehault, J.; Buntinx, G.; Huvenne, J.-P. *J. Phys. Chem. A* **2008**, *112*, 224.